Parameterization of Triangulated Surface Meshes based on Constraints of Distortion Energy Optimization

Junxiao Xue, Qingbin Li, Chengming Liu, Mingliang Xu

PII: S1045-926X(17)30287-2
DOI: 10.1016/j.jvlc.2018.01.002
Reference: YJVLC 826

To appear in: *Journal of Visual Languages and Computing*

Received date: 20 December 2017
Accepted date: 19 January 2018

Parameterization of Triangulated Surface Meshes based on Constraints of Distortion Energy Optimization

Junxiao Xue[1], Qingbin Li[2], Chengming Liu[1], Mingliang Xu[3]

1 School of Software, Zhengzhou University,Zhengzhou, 450000, China
2 Department of Mathematics and Physics, Zhengzhou Institute of Aeronautical Industry Management, Zhengzhou, 450046, China
3 School of Information Engineering, Zhengzhou University, Zhengzhou, 450000, China

Abstract

Parameterization of triangulated surface meshes is a crucial problem in computer graphics, computer aided geometric design and digital geometric processing. This paper addresses the problem of planar parameterization, i.e., mapping a given triangulated surface onto a planar domain. We construct an optimized algorithm for parameterization of genus-zero meshes and aim to minimize the distortion of the parameterization. An energy functional is proposed in the paper, that quantities angle and area distortions simultaneously, while the relative importance between angle and area preservation can be controlled by the user through a parameter. The method is based on an iterative procedure that incrementally flattens mesh by growing region to obtain a parameterization result with free boundary. The result is then converted to a parameterization with regular boundary by conformal mapping. Application of the method to texture mapping is presented. Experiments show that the proposed method can obtain better results than some common parameterization methods.

Keywords: Triangular Mesh, Parameterization, Conformal Mapping

1. Introduction

With the development of computer technology and 3D acquisition technique, 3D geometric data has become the fourth most important multimedia data type after the voice, image, and video. 3D triangular mesh is a simple, flexible technique and widely supported by graphics hardware. Therefore, a large number of applications of 3D triangular meshes can be found in computer graphics and computer-aided design.

A triangular mesh in 3D space can be represented by $\mathcal{S} = \mathcal{S}(\mathcal{G}, \boldsymbol{X})$, where $\boldsymbol{X} = \{\mathbf{x}_i = (x_i, y_i, z_i), i = 1, \ldots, N\}$ is the points set, $\mathcal{G} = \mathcal{G}(V, E, F)$ is a planar simply connected graph, $V = \{i : i = 1, \ldots, N\}$ is the point subscript set, E is the edge subscript set, and F is the face subscript set.

In general, working on general meshes is a difficult task because of their complicated geometry. The complicated geometry influences applications such as texture mapping, morphing and surface fitting. To overcome these problems, a common practice is to parameterize the 3D surface meshes onto a simple parameter domain so as to simplify the computations. For instance, textures can be designed on the simple domain and then mapped back onto the original surfaces[1,2,3,4]. It is also common to perform mesh morphing with the aid of algorithm to parameterize surface meshes over simple base domains[5,6]. Another example that usually makes use of parameterization is surface reconstruction[7,8,9]. With the development of the computer industry, the problem of finding a good parameterization method is becoming increasingly important.

3D triangular mesh parameterization refers to an isomorphic mapping from the triangular mesh in 3D space to a suitable parameter domain, which can be a flat area, sphere and so on. Triangular mesh parameterization has important applications in computer graphics and computer aided geometric design, such as for texture mapping, surface fitting, and surface reconstruction. Additionally, in the field of digital geometry processing, tasks such as 3D mesh editing, computer animation, multi-resolution analysis, and geometry compression require a prior parameterization of a 3D mesh to an easy area for interactive processing parameters.

Mathematically, parameterization mapping can be defined as

$$\phi : \mathcal{S} \to \mathcal{P}$$

where $\mathcal{S}$ is the triangular mesh in 3D space, and $\mathcal{P} = \mathcal{P}(\mathcal{G}_1, \boldsymbol{U})$ is a planar triangular mesh which is isomorphic to $\mathcal{S}$(Figure 1).

Ideally, the parameterization mapping between the 3D mesh and the planar mesh should be isometric, which means angles and distances are preserved. However, except for developable surfaces, general open surfaces cannot achieve this ideal condition. It has been shown by Gauss in 1828 that it is not possible to find an isometric mapping between two surfaces with different intrinsic curvature. To make a parameterization useful and applicable, one

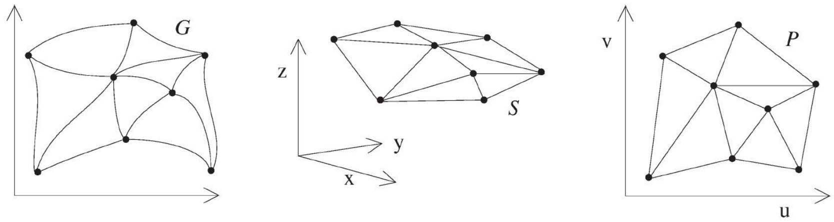

Figure 1: A graph, a triangular mesh, and parameterization

should seek for a method that minimizes certain types of distortions. In particular, it is desirable to minimize the angular distortions of the 3D meshes. Angle preserving parameterizations, also known as conformal parameterizations, effectively preserve the local geometry of the surfaces [10]. Therefore, in this paper, we attempt to develop an efficient conformal parameterization method by minimizing the distortion energy. In general, the choice of the parameter domain is a key factor in deciding the parameterization scheme. For simply-connected open surfaces, one popular choice of the parameter domain is the unit disk or square region. We present a parameterization algorithm which traverses the mesh using a region growing scheme. The algorithm takes into consideration of the distortion by two factors: area and angle, thus yielding results with less global distortion.

The rest of the paper is organized as follows. In Section 2, we review the previous surface parameterization techniques that are related to our work. In Section 3, we provide a brief sketch of mathematical theory related to this paper. Our proposed method is explained in details in Section 4. In Section 5, we present numerical experiments to demonstrate the effectiveness of our proposed method. The paper is concluded in Section 6.

2. Related Work

With a large variety of real applications, surface parameterization has been extensively studied by different researchers. Readers are referred to [11,12] for surveys of mesh parameterization methods. In this section, we will only give an overview of the works on conformal parameterization that are related to our work.

The parameterization of a triangular 3D mesh, which provides a bijective mapping between the mesh and a triangulation of a planar polygon, plays an important role in texture mapping. Floater[13] investigates a graph theory based parameterization for tessellated surfaces for the purpose of smooth surface fitting; his parameterization (actually a planar triangulation) is the solution of linear systems based on a convex combination. In[14], Hormann and Greiner use Floater's algorithm as a starting point for a highly non-linear local optimization algorithm which computes the positions for both interior and boundary nodes based on local shape preservation criteria. They called their approach: Most Isometric Parameterizations(MIPS). The method is promising, but it is not clear if the procedure is guaranteed to converge to a valid solution.

Wolfson et al.[15] introduce a flattening method based on the geodesic distance. They first use a computationally intensive method for finding the geodesic distance between pairs of points on the surface. Then, they use a specific MDS[16] (Multi-Dimensional Scaling) approach to flatten the surface using these geodesic distances, and by minimizing the function presented by Sammon in[17]. The work by Zigelman et al.[18] analytically finds an embedding of an open mesh in the plane by a MDS (Multi-Dimensional Scaling) method that optimally preserves the geodesic distances between mesh vertices. However, finding minimal geodesic distances between points on a continuous surface is a classical and difficult problem in differential geometry. All the methods above involve high computational complexity.

The angle based flattening (ABF) method presented by Sheffer et al.[19] is based on the observation that the set of angles of a 2D triangulation uniquely defines the triangulation up to global scaling and rigid transformations. They define an angle preservation metric directly in terms of angles. The method first computes the parameterization in angle space and subsequently converts it into 2D coordinates. In addition to avoiding flips, its important advantage is that it also closely preserves the angles and produces parameterizations with low area (and stretch) deformation. However, the optimization procedure used by ABF is numerically expensive. Recently, researchers have discussed methods to speed up ABF but an implementation is still lacking.

Some parameterization methods are based on strain-energy minimization[20]. They assume that the original 3D surface has zero energy, i.e. they are without wrinkles or stretches, while the 2D pattern is sought that minimizes the deformation energy. Their non-linear optimization scheme handles around a thousand vertices within a few seconds . Due to the limitation of the irregular mesh utilized in the above algorithms, the anisotropic material is hardly simulated. In[21] Wang et al. demonstrate the utilization of a wovenlike regular quadrilateral mesh model which greatly facilitates the simulation of anisotropic material based surface flattening.

Conformal maps preserve both the magnitude and sense of angles between arbitrary arcs. Thus, angle preservation is typically addressed from the conformal point of view. B. Lévy et al.[22] give a quasi-conformal parameterization method, based on a least squares approximation of the Cauchy-Riemann equations. The objective function minimizes angle deformation. In addition, N. Ray and B. Lévy[23] introduce HLSCM (Hierarchical Least squares Conformal Map), an efficient parameterization method for large meshes. The work by Gu[24] and Steven Haker et al.[25] have created flattened representations or visualizations of the cerebral cortex or cerebellum. These works indicate that if a quasi-length and area-preserving mapping is desired, the conformal mapping technique is a very reasonable starting point, since it preserves local geometry.

Aigerman et al.[26] introduces an algorithm for computing low-distortion, bijective mappings between surface meshes. Smith et al.[27] present a method for generating surface parameterizations from triangulated 3D surfaces partitioned into charts by using a distortion metric that prevents local folds of triangles in the parameterization. Others[28,29] bound the distortion of triangles to guarantee locally injective parameterizations. In addition, all of these methods can guarantee a bijective map if the user constrains the boundary of the charts to form a non-intersecting curve.

3. Brief Sketch of Mathematical Theory

In this section we review the required mathematical background essential for the parameterization method presented in this paper.

3.1. Conformal Mapping

Conformal mapping uses complex function to transform 2D domains (Figure 2).

A mapping is conformal if it preserves the angle between two differentiable arcs. To show that the mapping affected by a regular analytic function is indeed conformal, we proceed as follows. Suppose $f(z)$ is regular in the neighborhood of a point $z = z_0$ at which $f'(z_0) \neq 0$. The point $z = z_0$ is the terminal of two differentiable arcs α and β, the angle between their tangent vectors $\alpha'(z)$ and $\beta'(z)$ at point z_0 is the same as the angle between the tangent vectors $(f \circ \alpha)'(z_0)$ and $(f \circ \beta)'(z_0)$, i.e. the image of α and β

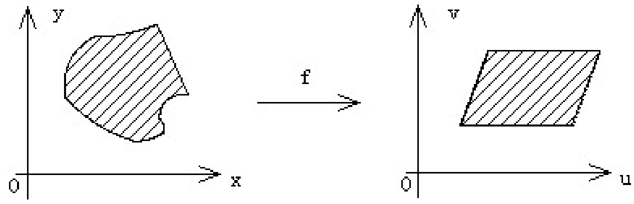

Figure 2: Sketch map of Conformal mapping

under f. This means that f is conformal at point z_0. If f is conformal for all points in D it is called a conformal mapping, which is equivalent to the Cauchy-Riemann equation such that:

$$\frac{\partial f}{\partial \overline{z}} = 0 \tag{1}$$

Consider now $z = x + iy$ and $w = u + iv$, we deduce a 2D function $f(x, y)$ from the function $w = f(z)$, parameterized by (x, y) that returns a 2D point (u,v). The Cauchy-Riemann equation is that:

$$\frac{\partial f}{\partial x} + i\frac{\partial f}{\partial y} = 0 \tag{2}$$

The existence of a conformal mapping between any two simply connected regions is guaranteed by the Riemann mapping theorem. Conformal mapping has long been used to solve boundary value problems in fluid flow, electrostatics, heat transfer, and elasticity. Recently, it has also been widely used in the fields of computer graphics and computer vision [24].

3.2. Differential Geometry

As mentioned above, parameterization is a isomorphic mapping between the 3D surface mesh and the target domain. The properties of the parameterization is closely related to the properties of the isomorphic mapping.

Consider the parametric surface $S : X(u, v) = (x(u, v), y(u, v), z(u, v))$. If S is differentiable, then its partial derivatives are:

$$X_1 = \tfrac{\partial X}{\partial u}, X_2 = \tfrac{\partial X}{\partial v}$$

The first fundamental form of S is

$$I = X_1 \cdot X_1 du^2 + 2X_1 \cdot X_2 dudv + X_2 \cdot X_2 dv^2. \tag{3}$$

Many properties of a parametric surface can be characterized by its first fundamental form.
Suppose:

$$g_i j = X_i \cdot x_j, i = 1, 2, j = 1, 2,$$

then we can define the matrix:

$$G = \begin{pmatrix} g_{11} \& g_{12} \\ g_{21} \& g_{22} \end{pmatrix} \tag{4}$$

Then, the first fundamental form of S can also be defined as the following:

$$I = (du \quad dv) G \begin{pmatrix} du \\ dv \end{pmatrix} \tag{5}$$

The determinant of G is:

$$g = g_{11} * g_{22} - g_{12} * g_{21}. \tag{6}$$

The formula (6) is referred to as the discriminant of the first fundamental form of the parametric surface.

For two parametric surfaces, we can always make their corresponding points have the same parameters through parameter transformation. Given two parametric surfaces S and S_1, assume that their corresponding points have the same parameters.

Proposition. The necessary and sufficient condition for the mapping between two parametric surfaces S and S_1 being conformal, is that their first fundamental forms are proportional, that is $I_1 = \lambda(u, v)I$, where $\lambda(u, v) \neq 0$.

That is if a mapping between two surfaces S and S_1 keeps local angles unchanged, then the mapping is conformal (angle-preserving).

Proposition. The necessary and sufficient condition for the mapping between two parametric surfaces S and S_1 being equiareal is that the determinants of their first fundamental forms are the same, that is $g = g_1$.

That is if a mapping between two surfaces S and S_1 keeps the areas unchanged, then the mapping is equiareal (area-preserving).

Proposition. The necessary and sufficient condition for the mapping between two parametric surfaces S and S_1 being isometric is that their first fundamental forms are the same, that is $I = I_1$.

That is if a mapping between two surfaces keeps curve lengths unchanged, then the mapping is isometric.

Obviously, any isometric mapping is conformal and equiareal, and every mapping that is conformal and equiareal is also isometric. This can be expressed as:

$$isometric \Longleftrightarrow conformal + equiareal.$$

4. Proposed Method

In this section, we present our proposed method for disk conformal parameterizations of simply-connected open surfaces in details.

4.1. Validity of parameterization

Parameterization of triangular mesh must meet the requirements of validity. The necessary and sufficient condition for the validity is that the vertices, edges and faces of the original triangular mesh and the parametric triangular mesh must have one-to-one correspondence. The corresponding edges must connect the corresponding vertices and the corresponding faces must be connected at the corresponding vertices and edges. Additionally, the boundary vertices of the original triangle mesh and the parametric triangular mesh should have counterclockwise correspondence. As shown in Figure 3, u is a valid parameter of X, and u^* is invalid.

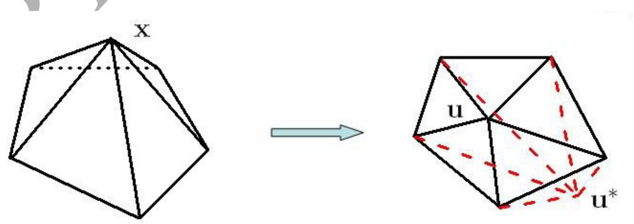

Figure 3: Validity of Parameterization

4.2. Parameterization Distortion

Although the parameterization of a surface mesh is not unique, the process of obtaining the best parameterization with respect to a certain criteria is a challenging problem. In fact, along with meeting the criteria of validity, parameterization must also meet the requirements of distortion minimization. Apart from these intrinsic surface properties, there are other properties which depend on the parameterization - most importantly, the distortion of the intrinsic geometric metrics (such as length, angle or area). Mathematically, if the parameterization between the 3D triangular mesh and the plane is isometric, the requirements are naturally satisfied. However, we can just get an isometric mapping between the developable surface whose Gauss curvature is 0 and the plane. For a general surface mesh, the distortion of the parameterization is inevitable.

4.3. Distortion Energy

For our application, since the parameterization mapping is isomorphic, we are looking for an inverse mapping form. Suppose $T = \Delta p_1 p_2 p_3$ is a spatial triangle, and $T' = \Delta q_1 q_2 q_3$ is a planar triangle, where $q_i = (u_i, v_i), i = 1, 2, 3$. For the mapping $f : T' \to T$, if f satisfies the Cauchy-Riemann equation(2), it is angle-preserved.

We define the angle-preserved energy as

$$E_1(T) = |\frac{\partial f}{\partial u} + i\frac{\partial f}{\partial v}|^2. \tag{7}$$

where $|\cdot|$ is gradient.

Consider the first basic form matrix of f:

$$I = \begin{pmatrix} \frac{\partial f}{\partial u} \cdot \frac{\partial f}{\partial u} & \frac{\partial f}{\partial u} \cdot \frac{\partial f}{\partial v} \\ \frac{\partial f}{\partial u} \cdot \frac{\partial f}{\partial v} & \frac{\partial f}{\partial v} \cdot \frac{\partial f}{\partial v} \end{pmatrix}.$$

The mapping is area-preserved if $detI \equiv 1$. So we define the angle-preserved energy as:

$$E_2(T) = |detI - 1|^2. \tag{8}$$

Based on equation (7) and (8), we define the distortion energy as:

$$E(T) == \varepsilon \cdot |\frac{\partial f}{\partial u} + i\frac{\partial f}{\partial v}|^2 + (1 - \varepsilon) \cdot |detI - 1|^2. \tag{9}$$

where $\varepsilon \in [0, 1]$. Equation (9) is a linear combination of equation (7) and (8), so it can measure the angular distortion and area distortion associated with the parameterization mapping.

The problem can be reduced to $R^2 \rightarrow R^2$ by considering how to map the triangles of a 3D mesh to their corresponding triangles in the u-v plane in parameter space. In the following section, we will create a discretized form of equation (9) by converting each 3D triangle to its local 2D coordinate frame.

4.4. Discretization

We propose a discretization form of equation (9) in the following. Consider the spatial triangle $T = \Delta p_1 p_2 p_3$, where $p_i = (\bar{x_i}, \bar{y_i}, \bar{z_i}), i = 1, 2, 3$. Suppose $\overrightarrow{A} = p_2 - p_1, \overrightarrow{B} = p_3 - p_1$, and $N = A \times B / \parallel A \times B \parallel, X = N \times B / \parallel N \times B \parallel, Y = X \times B / \parallel X \times B \parallel$, then X and Y is a local basis of T(figure 4).

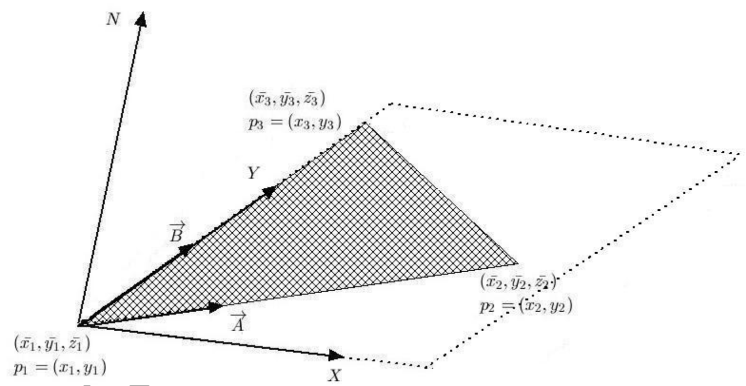

Figure 4: Triangle's Local Coordinate System

On the basis of X and Y, we can get $p_1 = (0, 0), p_2 = (A \cdot X, A \cdot Y), p_3 = (B \cdot X, B \cdot Y)$.

Based on this idea, we can use the reconstructed 3D points to form a mesh $M = \{p_i, i \in [1, n], T_j, j \in [1, m]\}$. Here p_i are the n 3D points on the surface mesh which serve as the vertices, and T_j represents the resulting m triangles, denoted as a tuple of three mesh vertices. In their local coordinate frame, we can consider $p_i = (x'_i, y'_i)$.

A triangle-to-triangle mapping is defined by a unique affine transformation between the original and destination triangle. For the planar triangle $T' = \Delta q_1 q_2 q_3$, where $q_i = (u_i, v_i), i = 1, 2, 3$. Consider the mapping $f : T' \to T$, if $f(q_i) = p_i, i = 1, 2, 3$, then

$$f(q) = \frac{Area(\Delta q q_2 q_3)p_1 + Area(\Delta q_1 q q_3)p_2 + Area(\Delta q_1 q_2 q)p_3}{Area(\Delta q_1 q_2 q_3)},$$

where $Area(\cdot)$ is the area of the triangle. The partial derivatives (triangle gradient) of this equation are as follows:

$$\begin{cases} \dfrac{\partial f}{\partial u} = \dfrac{(v_2 - v_3)p_1 + (v_3 - v_1)p_2 + (v_1 - v_2)p_3}{2Area(\Delta q_1 q_2 q_3)}, \\ \dfrac{\partial f}{\partial v} = \dfrac{(u_3 - u_2)p_1 + (u_1 - u_3)p_2 + (u_2 - u_1)p_3}{2Area(\Delta q_1 q_2 q_3)}. \end{cases} \tag{10}$$

The triangle gradient (10) can be used to formulate the Cauchy-Riemann equations. This can be written compactly in the matrix form as follows:

$$\begin{bmatrix} \frac{\partial u}{\partial x} - \frac{\partial v}{\partial y} \\ \frac{\partial v}{\partial x} + \frac{\partial u}{\partial y} \end{bmatrix} = \frac{1}{2A_T} \begin{bmatrix} \Delta x_1 & \Delta x_2 & \Delta x_3 & -\Delta y_1 & -\Delta y_2 & -\Delta y_3 \\ \Delta y_1 & \Delta y_2 & \Delta y_3 & \Delta x_1 & \Delta x_2 & \Delta x_3 \end{bmatrix} \begin{bmatrix} u_1 \\ u_2 \\ u_3 \\ \dots \\ v_1 \\ v_2 \\ v_3 \end{bmatrix} = \begin{bmatrix} 0 \\ 0 \end{bmatrix} \tag{11}$$

where $\Delta x_1 = (x_3 - x_2), \Delta x_2 = (x_1 - x_3), \Delta x_3 = (x_2 - x_1)$ and Δy_i is defined similarly, A_T is the area of the triangle defined by $T_{p_1 p_2 p_3}$. Solving this equation will find the appropriate parameters (u_i, v_i). Working from the equation (11), we can write a global system of equations, $AX = b$, that incorporates all the vertices and triangles in the mesh T.

4.5. Solving the System

To obtain a unique solution for the system $AX = b$ up to a similitude, some vertices must be constrained - otherwise the (u_i, v_i) could have any arbitrary orientation in the 2D plane. Fixing at least two values will give a unique solution and constrains the orientation in the resulting conformal map. For example, if we want to constrain l vertices, p_k, to map to specified locations q_k, we modify the matrix A and vector b to reflect this constraint, such that $A's$ l column entries, a_k and a_{2k}, are removed from the matrix A.

A new b is constructed to incorporate this constraint in the solution, such that:

$$b = -\begin{bmatrix} a_{2k_1} & a_{2k_2} & \dots & a_{lk_1} & a_{lk_2} \end{bmatrix} \begin{bmatrix} u_{k_1} \\ \vdots \\ u_{k_l} \\ v_{k_1} \\ \vdots \\ v_{k_l} \end{bmatrix},$$

where a_i are the columns removed from A, and u_{ki} and v_{ki} represent the constrained parameter values.

After computing the new A and b, we can solve the linear system. Since the solution is exact for minimizing the parameterization distortion, the vector x is computed to minimize $\|Ax - b\|^2$. This linear system can be solved using sparse solvers such as Conjugate Gradient. The resulting x vector contains the corresponding (u, v) values for the parameterization.

4.6. Algorithm

We consider a bounded connected triangular mesh patch which is homeomorphic to a disk. Firstly, we arbitrarily select a triangle T_0 and put it on the planar domain with no distortion. Then we flatten all of the other triangles by minimizing the distortion energy. The algorithm is explained step by step as follows:

Input: 3D Mesh $\mathcal{S}$, which is bounded and simply-connected.

Output: Planar mesh $\mathcal{P}$, which is approximately isometric to mesh $\mathcal{S}$.

Step 1. Read the data, store the coordinates of the vertices and the index array.

Step 2. Select a seed triangle T_0 from $\mathcal{S}$; embed it onto the plane with no distortion. And initialize the front-patch array as the three edges of the seed triangle.

Step 3. Examine all the triangles adjacent to the front-patch, and embed them onto the plane by minimizing the distortion energy.

Step 4. If the vertex in Mesh $\mathcal{P}$ have more than one corresponding vertices in the planar domain, unify them into one.

Step 5. If all the vertices of the Mesh $\mathcal{S}$ have been checked, the program stops. If not, redefine the front-patch array, and go to step 3.

The key problem in the algorithm is to compute the minimization of the distortion energy in step 3. The problem can be solved using sparse solvers such as Conjugate Gradient. Additionally, the boundary of parameterization by the algorithm is free. If we want to obtain a result with a regular boundary, we can get it by a $2D \to 2D$ conformal mapping.

For a given region with polygonal boundary, a general method of constructing the conformal mapping is offered by Schwarz-Christoffel transformations.

Theorem Suppose there is a polygon Δ with complex vertices (possibly infinite) $w_1, w_2, \cdots, w_n$, given in counter-clockwise order. To each vertex w_k $(k = 1, 2, \cdots, n)$ there is a corresponding interior turning angle $\alpha_k \pi$ $(k = 1, 2, \cdots, n)$, where $0 < \alpha_k < 2$. Then every function which maps a unit disk conformally onto the interior of Δ and satisfies $f(0) = a$ can be expressed in the form

$$f(z) = a + c \int_0^z \prod_{k=1}^{n} (1 - \frac{z}{z_k})^{\alpha_k - 1} dz, \tag{12}$$

where c is a suitable complex constant, z_k are the pre-vertices of w_k with $|z_k| = 1, (k = 1, 2, \cdots, n)$. The map f may be made unique by requiring that $f'(0) = c$ be positive, or by prescribing the position of one pre-vertex z_k.

We denote the map $f(z)$ as a disk-map. A map between two polygons can be obtained by using a composite map which consists of one forward and one inverse disk-map. Regard the pre-vertices z_k $(k = 1, 2, \cdots, n)$ in formula (12) as the *parameters* of the Schwarz-Christoffel mapping function. The Schwarz-Christoffel formula is mathematically appealing, but problematic in practice. The main practical difficulty with the formula (12) is that except in special cases, the pre-vertices z_k $(k = 1, 2, \cdots, n)$ cannot be computed analytically. This is the Schwarz-Christoffel parameter problem, and its solution is the key problem in any Schwarz-Christoffel map. Once the parameter problem is solved, the multiplicative constant c can be found and the Schwarz-Christoffel formula is the explicit representation of the mapping function f. Though the Schwarz-Christoffel parameter problem cannot be computed analytically, its solution can be numerically solved by the Schwarz-Christoffel toolbox[30] in MATLAB, which is well suited for the interactive computation of Schwarz-Christoffel mappings.

The effective parameterization must ensure that there is no self-intersection, i.e., all triangles in a planar domain must not fold-over. The original 3D triangular mesh $\mathcal{S}$ is a two-dimensional manifold. In the process of parameterizing $\mathcal{S}$, if there is no triangle inversion (triangle-flipping), the 2D triangular mesh $\mathcal{P}$ obtained by parameterizing may not overlap - meaning the sequence order of the three vertices of the 2D triangle is the same as the original 3D triangle.

Proposition. Given a triangle $T = \Delta p_1 p_2 p_3 \in 3D$, the coordinates of the vertices in the local orthogonal basis are $p_i = (x_i, y_i), i = 1, 2, 3$. Suppose the mapping $f : T \to T'$, where $T' = \Delta q_1 q_2 q_3 \in 2D$, and $q_i = (u_i, v_i), i = 1, 2, 3$. If f satisfies the Cauchy-Riemann equation

$$\frac{\partial f}{\partial x} + i\frac{\partial f}{\partial y} = 0, \tag{13}$$

then T' will not be flipped.

Proof:. Equation(13) is equivalent to $\frac{\partial u}{\partial x} = \frac{\partial v}{\partial y}, \frac{\partial u}{\partial y} = -\frac{\partial v}{\partial x}$, thus, the determinant of the Jacobi matrix of mapping f satisfies:

$$|J_f| = \begin{vmatrix} \frac{\partial u}{\partial x} & \frac{\partial u}{\partial y} \\ \frac{\partial v}{\partial x} & \frac{\partial v}{\partial y} \end{vmatrix} = \frac{\partial u}{\partial x} \cdot \frac{\partial v}{\partial y} - \frac{\partial v}{\partial x} \cdot \frac{\partial u}{\partial y} = (\frac{\partial u}{\partial x})^2 + (\frac{\partial u}{\partial y})^2 \geq 0,$$

So the sequence order of the vertices of the triangle stays unchanged after the mapping, that is, T' will not be flipped.

5. Experiments

The methods presented in this paper have been implemented and tested on several mesh models. Figure 5 is the parameterization of the nose mesh, and figure 6 is the parameterization of the face mesh. We take figure 3 as an example to illustrate the process of parameterization. In figure 5, figure 5 (a) is the original triangular mesh surface. We use the deformation energy optimization method based on the regional growth algorithm to flatten Figure 5 (a) onto the planar domain. Then we get a free boundary parameterization result (figure 3 (b)). Next, we extract the polygon boundary of figure 5 (b) , and use the Schwarz-Christoffel formula to construct a 2D→2D conformal mapping to map the free boundary parameterization to a unit square domain (figure 5 (c)) . In fact, other regular boundary (such as the unit circle etc.) parameters can also be obtained by using a similar process. Figures 5 (d) to 5 (f) were obtained by the uniform parameterization method, conformal parameterization method and mean coordinate parameterization method respectively. From the figures we can see that the results obtained by distortion energy optimization method is very similar to the results obtained by the other methods.

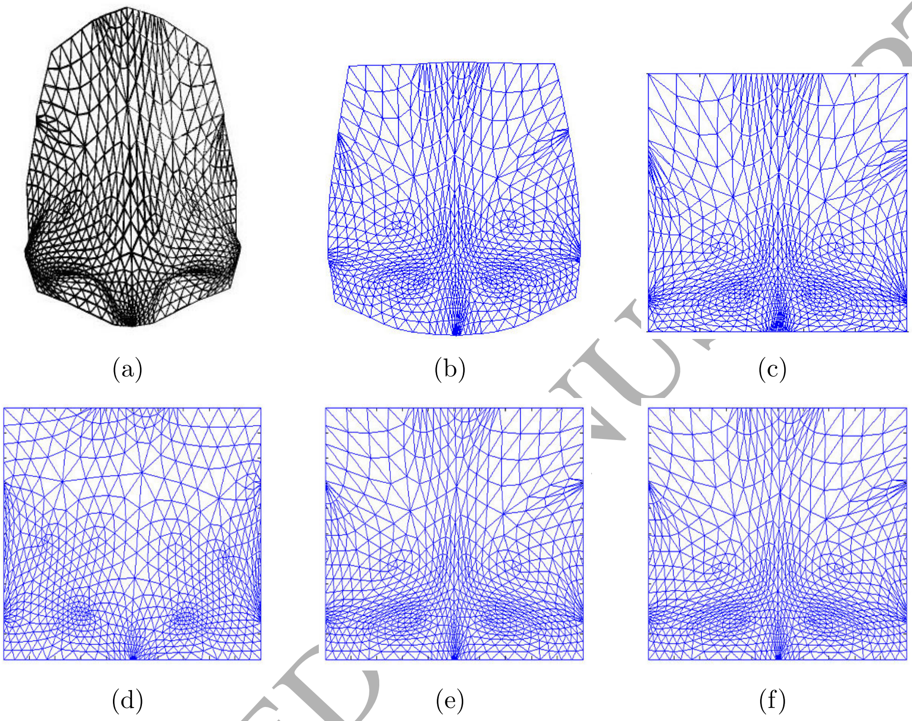

Figure 5: Nose Mesh Parameterization. (a) original mesh; (b) free-boundary parameterization based on distortion energy optimization; (c) regular-boundary parameterization based on distortion energy optimization; (d) uniform parameterization; (e) conformal parameterization; (f) mean value coordinate parameterization

Texture mapping is one technique that can be used to examine the effect of the parameterization method. Figures 7 and 8 illustrate the texture mapping results based on the parameterization method proposed in this paper. We can see that the textures in figure 7 and figure 8 are uniform and satisfactory. In figure 9 and figure 10, we apply several other parameterization methods to the same texture to compare their results with the method proposed in the paper. Specifically, figure 10(a)-(c) are the Beijing opera mask texture mapping results based on the uniform parameterization method, the conformal parameterization method, the mean-value coordinate parameterization method and the distortion energy optimization parameterization method re-

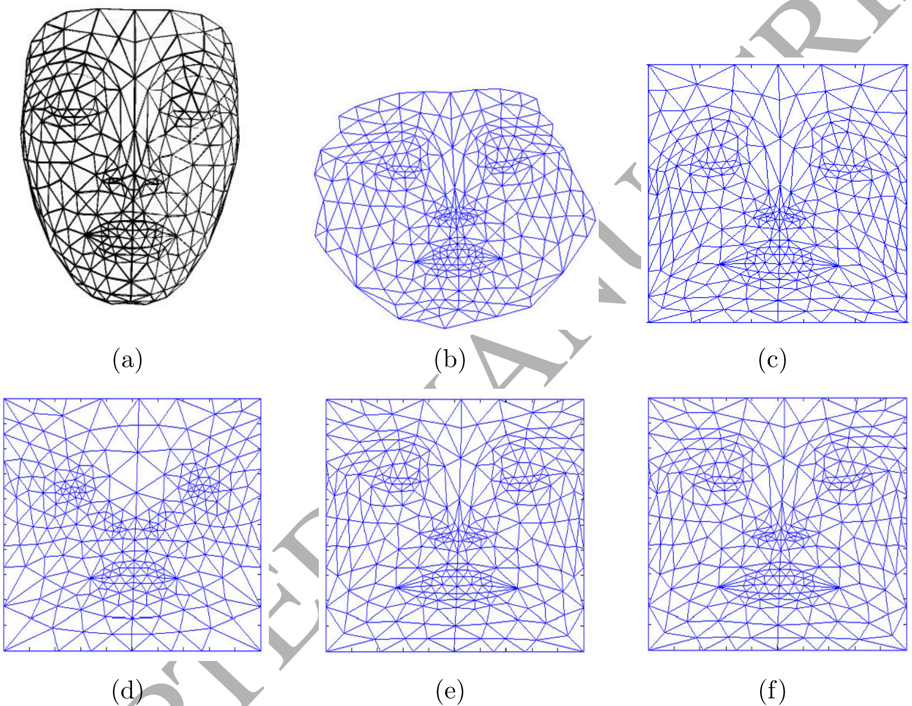

Figure 6: Face Mesh Parameterization. (a) original mesh; (b) free-boundary parameterization based on distortion energy optimization; (c) regular-boundary parameterization based on distortion energy optimization; (d) uniform parameterization; (e) conformal parameterization; (f) mean value coordinate parameterization

spectively. And figure 10(d)-(f) are the local details of figure 10(a)-(c). We can observe that the result based on the distortion energy optimization parameterization method is best.

(a) (b) (c)

Figure 7: Texture Mapping on Nose. (a) original model; (b) chessboard; (c) I-Love-China.

Texture mapping is a method to measure the distortion of parameterization visually. We also define two kinds of quantitative criteria to measure the distortion of parameterization.

Firstly, we measure the parametric distortion with the mean relative deviation of area and angle between the original mesh and the parameterized mesh. The mean deviations are defined as:

$$L_A^2(\mathcal{P}) = \sqrt{\sum_{j\in F}\Big[\frac{\mathcal{A}(T_j)}{\sum\limits_{T_j\in\mathcal{S}}\mathcal{A}(T_j)} - \frac{\mathcal{A}(T_j^*)}{\sum\limits_{T_j^*\in\mathcal{P}}\mathcal{A}(T_j^*)}\Big]^2}, \tag{14}$$

and

$$L_B^2(\mathcal{P}) = \sqrt{\sum_{j\in F}\Big[\sum_{i=1,2,3}\Big[\frac{\mathcal{S}(A_{i,j})}{2\pi} - \frac{\mathcal{S}(A_{i,j}^*)}{2\pi}\Big]^2\Big]}. \tag{15}$$

where $L_A^2(\mathcal{P})$ is a metric of the mean deviation of area, $L_B^2(\mathcal{P})$ is a metric of the mean deviation of angle. $\mathcal{A}(\cdot)$ is the area of the triangle T_j, $\mathcal{S}(\cdot)$ is an angle metric.

Similarly, we measure the parametric distortion with the maximum relative deviation of area and angle between the original mesh and the parame-


(a)


(b)


(c)


(d)


(e)


(f)

Figure 8: Texture Mapping on Face. (a)-(f) Beijing Opera Face texture

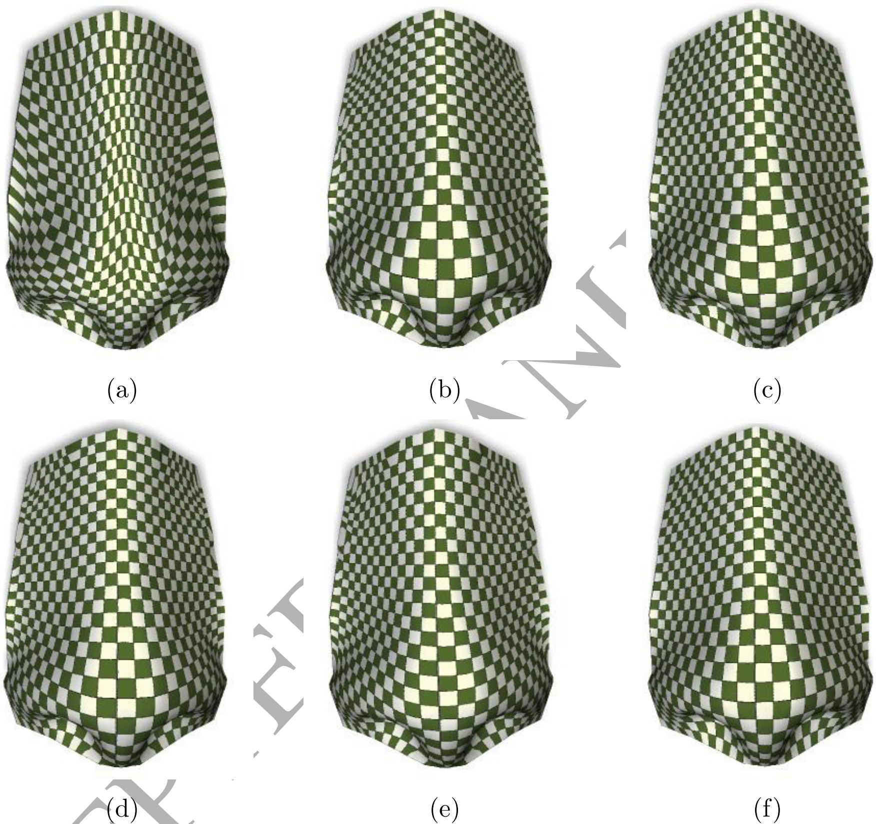

Figure 9: Comparison of texture mapping obtained from different parameterization methods. (a) uniform parameterization; (b) conformal parameterization; (c) mean-value coordinate parameterization; (d) harmonic mapping parameterization; (e) intrinsic parameterization; (f) distortion energy optimization parameterization

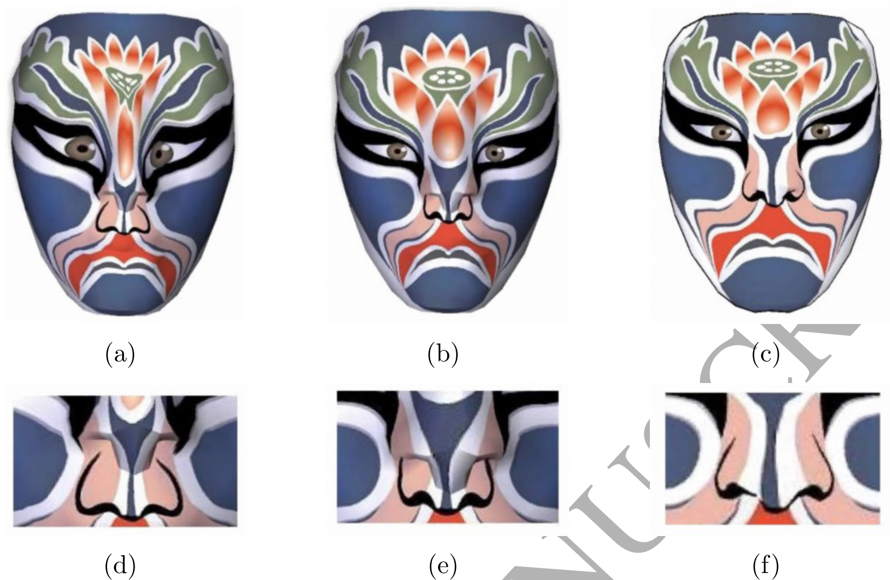

Figure 10: Comparison of texture mapping obtained from different parameterization methods. (a) uniform parameterization; (b) mean-value coordinate parameterization; (c) distortion energy optimization parameterization; (d)-(f) local details

terized mesh. The maximum deviations are defined as:

$$L_A^\infty(\mathcal{P}) = \max_{j\in F}(|[\frac{\mathcal{A}(T_j)}{\sum\limits_{T_j\in\mathcal{S}}\mathcal{A}(T_j)} - \frac{\mathcal{A}(T_j^*)}{\sum\limits_{T_j^*\in\mathcal{P}}\mathcal{A}(T_j^*)}|), \tag{16}$$

and

$$L_B^\infty(\mathcal{P}) = \max_{j\in F}([\sum_{i=1,2,3}[\frac{\mathcal{S}(A_{i,j})}{2\pi} - \frac{\mathcal{S}(A_{i,j}^*)}{2\pi}]^2). \tag{17}$$

where $L_A^\infty(\mathcal{P})$ is a metric of the maximum deviation of area and $L_B^\infty(\mathcal{P})$ is a metric of the maximum deviation of angle.

By using the metric defined in equation 14-17, we quantitatively compare the area distortion and the angle distortion of the nose mesh model and the human face mesh model with different parameterization methods. In table 1 and table 2, A represents the results of uniform parameterization, B represents the results of conformal parameterization, C represents the results of the mean value coordinate parameterization, D represents the results of equidistant energy optimization parameterization of free boundary, and E represents the results of equidistant energy optimization parameterization of regular boundary. From the statistical data in the tables, we can see that the area and angle distortions of the uniform deformation is large, while the energy optimization parameters of the corresponding isometric deformation is small compared to the conformal parameters, and the mean value coordinate parameters, and the free boundary offset optimization is the minimum deformation energy parameter.

In the use of conformal transformation 2D between regions will transform the free boundary parameterization for parametric boundary rules, because near the boundary conformal nature of conformal transformation will be affected therefore, the parametric boundary rules would produce a certain angle deformation near the border area and deformation which compare with the parameterization of free boundary. So the distortion of the parameterization with regular boundary is larger than that of free boundary, and the relevant data in the table also confirms this point. However, in terms of the parameterization with regular boundary, the angle distortion of the results based on the algorithm presented in this paper is close to the conformal parameterization method and the mean value coordinate parameterization method, while the area distortion is far less than the above two methods. Overall, the method proposed in this paper has smaller distortions.

	L^2_{area}	L^2_{angle}	L^∞_{area}	L^∞_{angle}
A	4.0259	32.3802	1.6564	3.2481
B	0.0152	1.3537	0.0014	0.1022
C	0.0263	2.2204	0.0197	0.1654
D	0.0030	0.1456	0.0021	0.0037
E	0.0073	1.0784	0.0018	0.0373

Table 1: Statistical data of nose mesh parameterization distortion.

6. Conclusion

We have presented a novel method to parameterize triangulated surface meshes by minimizing the distortion energy. First of all, we introduced an energy function to measure the parameterization disortion based on the conformal mapping and the theory of differential geometry. Then, we obtained

	L^2_{area}	L^2_{angle}	L^∞_{area}	L^∞_{angle}
A	1.2441	16.317	0.0128	1.9124
B	0.0117	2.5086	0.0187	0.0289
C	0.0156	1.0029	0.0161	0.1524
D	0.0214	0.3001	0.0021	0.0163
E	0.0166	1.4889	0.0014	0.0377

Table 2: Statistical data of face mesh parameterization distortion.

the parameterization result by iteratively computing the minimizing solutions of the energy functions of the triangles at every layer. The method takes into consideration the angle distortion and area distortion, thus yielding results with less global distortion. Various experiments have been worked out to illustrate the effectiveness of the techniques proposed in this paper.

Acknowledgements

The work was supported by the National Key Research and Development Program of China under Grant No. 2017YFC0804401, the National Natural Science Foundation of China under Grant Nos. 61472370, 61672469, 61379079, 61322204, and 61502433, the Natural Science Foundation of Henan Province of China under Grant No. 162300410262, and the Key Research Projects of Henan Higher Education Institutions of China under Grant No. 18A413002.

References

1. Steven Haker, Sigurd Angenent, Allen Tannenbaum, Ron Kikinis, Guillermo Sapiro, and Michael Halle. Conformal surface parameterization for texture mapping. *IEEE Transactions on Visualization and Computer Graphics*, 6(2):181–189, 2000.

2. Eugene Zhang, Konstantin Mischaikow, and Greg Turk. Feature-based surface parameterization and texture mapping. *ACM Transactions on Graphics (TOG)*, 24(1):1–27, 2005.

3. Fabián Prada, Misha Kazhdan, Ming Chuang, Alvaro Collet, and Hugues Hoppe. Spatiotemporal atlas parameterization for evolving meshes. *ACM Transactions on Graphics (TOG)*, 36(4):58, 2017.

4. Marco Tarini, Cem Yuksel, and Sylvain Lefebvre. Rethinking texture mapping. In *ACM SIGGRAPH 2017 Courses*, page 11. ACM, 2017.

5. Aaron WF Lee, David Dobkin, Wim Sweldens, and Peter Schröder. Multiresolution mesh morphing. In *Proceedings of the 26th annual conference on Computer graphics and interactive techniques*, pages 343–350. ACM Press/Addison-Wesley Publishing Co., 1999.

6. Chao Peng and Sabin Timalsena. Fast mapping and morphing for genus-zero meshes with cross spherical parameterization. *Computers & Graphics*, 59:107–118, 2016.

7. Venkat Krishnamurthy and Marc Levoy. Fitting smooth surfaces to dense polygon meshes. In *Proceedings of the 23rd annual conference on Computer graphics and interactive techniques*, pages 313–324. ACM, 1996.

8. Michael S Floater and Martin Reimers. Meshless parameterization and surface reconstruction. *Computer Aided Geometric Design*, 18(2):77–92, 2001.

9. Linlin Xu, Ruimin Wang, Zhouwang Yang, Jiansong Deng, Falai Chen, and Ligang Liu. Surface approximation via sparse representation and parameterization optimization. *Computer-Aided Design*, 78:179–187, 2016.

10. Gary Pui-Tung Choi and Lok Ming Lui. A linear formulation for disk conformal parameterization of simply-connected open surfaces. *Advances in Computational Mathematics*, pages 1–28, 2017.

11. Kai Hormann, Bruno Lévy, and Alla Sheffer. Mesh parameterization: Theory and practice. 2007.

12. Alla Sheffer, Emil Praun, Kenneth Rose, et al. Mesh parameterization methods and their applications. *Foundations and Trends® in Computer Graphics and Vision*, 2(2):105–171, 2007.

13. Michael S Floater. Parametrization and smooth approximation of surface triangulations. *Computer aided geometric design*, 14(3):231–250, 1997.

14. Kai Hormann and Günther Greiner. Mips: An efficient global parametrization method. Technical report, ERLANGEN-NUERNBERG UNIV (GERMANY) COMPUTER GRAPHICS GROUP, 2000.

15. Estarose Wolfson and Eric L Schwartz. Computing minimal distances on polyhedral surfaces. *IEEE Transactions on Pattern Analysis and Machine Intelligence*, 11(9):1001–1005, 1989.

16. Joseph B Kruskal and Myron Wish. *Multidimensional scaling*, volume 11. Sage, 1978.

17. John W Sammon. A nonlinear mapping for data structure analysis. *IEEE Transactions on computers*, 100(5):401–409, 1969.

18. Gil Zigelman, Ron Kimmel, and Nahum Kiryati. Texture mapping using surface flattening via multidimensional scaling. *IEEE Transactions on Visualization and Computer Graphics*, 8(2):198–207, 2002.

19. Alla Sheffer and Eric de Sturler. Parameterization of faceted surfaces for meshing using angle-based flattening. *Engineering with computers*, 17(3):326–337, 2001.

20. Chakib Bennis, Jean-Marc Vézien, and Gérard Iglésias. Piecewise surface flattening for non-distorted texture mapping. In *ACM SIGGRAPH computer graphics*, volume 25, pages 237–246. ACM, 1991.

21. Charlie CL Wang, Kai Tang, and Benjamin ML Yeung. Freeform surface flattening based on fitting a woven mesh model. *Computer-Aided Design*, 37(8):799–814, 2005.

22. Bruno Lévy, Sylvain Petitjean, Nicolas Ray, and Jérome Maillot. Least squares conformal maps for automatic texture atlas generation. In *ACM transactions on graphics (TOG)*, volume 21, pages 362–371. ACM, 2002.

23. Nicolas Ray and Bruno Levy. Hierarchical least squares conformal map. In *Computer Graphics and Applications, 2003. Proceedings. 11th Pacific Conference on*, pages 263–270. IEEE, 2003.

24. Xianfeng Gu, Yalin Wang, Tony F Chan, Paul M Thompson, and Shing-Tung Yau. Genus zero surface conformal mapping and its application to brain surface mapping. *IEEE Transactions on Medical Imaging*, 23(8):949–958, 2004.

25. Steven Haker, Sigurd Angenent, Allen Tannenbaum, Ron Kikinis, Guillermo Sapiro, and Michael Halle. Conformal surface parameterization for texture mapping. *IEEE Transactions on Visualization and Computer Graphics*, 6(2):181–189, 2000.

26. Noam Aigerman, Roi Poranne, and Yaron Lipman. Lifted bijections for low distortion surface mappings. *ACM Transactions on Graphics (TOG)*, 33(4):69, 2014.

27. Jason Smith and Scott Schaefer. Bijective parameterization with free boundaries. *ACM Transactions on Graphics (TOG)*, 34(4):70, 2015.

28. Renjie Chen and Ofir Weber. Bounded distortion harmonic mappings in the plane. *ACM Transactions on Graphics (TOG)*, 34(4):73, 2015.

29. Roi Poranne and Yaron Lipman. Provably good planar mappings. *ACM Transactions on Graphics (TOG)*, 33(4):76, 2014.

30. Tobin A Driscoll. Algorithm 756: A matlab toolbox for schwarz-christoffel mapping. *ACM Transactions on Mathematical Software (TOMS)*, 22(2):168–186, 1996.